RESEARCH ARTICLE

Image security of agricultural environment monitoring based on image encryption algorithm of secure compressed sensing

Jingyi Liu*

Department of Information Engineering, Yantai Vocational College, Yantai, Shandong, China

Received: March 22, 2023; **accepted:** April 22, 2023.

Agricultural environment monitoring is to track the residues and accumulation dynamics of pollutants in agricultural products to ensure the safety of agricultural products and human health, and to provide scientific basis for agricultural environment management. The development of network technology has enabled people to share agricultural information resources. However, the openness and sharing of agricultural information resources often brings about data security issues. In addition, the representative method of current monitoring image data is compressed sensing, which lacks effective security technology guarantee in the process of signal acquisition and transmission. Therefore, it is even more necessary to use encryption methods for optimization. Based on the diversity, complexity, and security of the image data, an adaptive algorithm was proposed in this study to realize the reconstruction optimization of compressed sensing technology and the processing of the detected image data. An image fusion algorithm was introduced to realize the differential processing of different frequency subbands. Blockchain technology was introduced into the sensing matrix to realize encryption processing and ensure the security of agricultural environment monitoring image data. The security application analysis of the proposed compressed sensing encryption algorithm showed that the average reconstruction probability of the proposed improved encryption algorithm was 84%, which was less affected by the number of measurements, and the overall fitness changed more smoothly. Moreover, the algorithm had a large signal-to-noise ratio in the reconstruction of agricultural environment images with different scale characteristics, and its scores in the five objective evaluation dimensions of image quality were better than other algorithms. The satisfaction of algorithm process encryption and image data security had reached 80.12% and 89.23%, respectively. This research enhanced and reconstructed the existing agricultural environment monitoring images to help agricultural environment monitoring and make up for the lack of security of agricultural environment monitoring images, which has a very important research value.

Keywords: compressed sensing; encryption algorithm; agricultural environment; reconstruction probability; blockchain.

***Corresponding author:** Jingyi Liu, Department of Information Engineering, Yantai Vocational College, Yantai 264670, Shandong, China. Email: liujingyi521@126.com.

Introduction

Agriculture is the basic industry supporting the construction and development of the national economy. Timely, effective, quantitative, and accurate dynamic monitoring of agricultural production and its spatial distribution has important significance and value. Agricultural environment, as an important element that affects crop production, has a close relationship with the overall development level of agriculture. The monitoring of agricultural environment refers to the intermittent or continuous determination of the concentration of pollutants

in the environment, and the control of the overall environmental quality through observation and analysis, and the timely and effective treatment of pollutants. The image data can reflect the changes of ground objects and environment. Most scholars have studied agricultural environmental monitoring. Sodjinou, *et al*. proposed a fast semantic segmentation algorithm, which could segment the color image of crops [1]. The accuracy of the algorithm segmentation exceeded 90%. The experimental results showed that the algorithm successfully provided accurate and convincing results for crop and weed segmentation in images with complex weeds. Liu, *et al*. developed an agricultural vegetation coverage extraction method based on K-means [2]. The algorithm could extract vegetation coverage information from gray image. The experimental results showed that the absolute error value of the algorithm was lower than 0.045 under different soil and time, and its performance was significantly higher than that of the pixel dichotomy. Chatterjee, *et al*. proposed a disease prediction method for agricultural and animal husbandry production, which predicted the disease of products through unsupervised classification [3]. The experimental results showed that the method had high accuracy, but its application range was small, and the target product needed to be further expanded. Bijandi, *et al*. developed a multi-objective artificial bee colony method [4], which defined different land models according to terrain and set geometry. The defined model was compared with the shape proposed by the designer, and the results showed that the shape and size of the algorithm could bring higher efficiency and better meet the agricultural conditions. Yousefi-Babadi, *et al*. designed a weight algorithm for arranging wheat storage measures based on geographic information system, which could plan wheat storage according to land use and logistics [5]. They conducted a case study in Iran, and the results showed that 16% of the counties were identified as sustainable locations for the relocation of wheat storage facilities, and the researchers also believed that the results were effective. With the advancement of the Internet of Things (IoT) in agriculture, more and more enterprises are integrating agricultural production with IoT technology, utilizing agricultural data to improve production efficiency and resource management level, thereby building modern agriculture and optimizing industrial upgrading. However, with the explosive development of the agricultural Internet of Things, a series of risks and drawbacks have been exposed such as data being intercepted by hacker sessions and address spoofing during transmission. Therefore, it is particularly important to ensure data security. Many algorithms have been applied in agricultural detection, but there are few studies on its security and encryption process.

The theory of compressed sensing makes it difficult for signal sampling to take useful signal data from a large amount of data, which leads to the generation of too much redundant information and increases the pressure of information storage. This theory includes sparse representation, sensor matrix, and reconstruction algorithm, and is applied in sensor networks, image imaging, detection and recognition, and other fields [6, 7]. The complexity and diversity of agricultural environment detection image data limits the effect of the original data sampling method, while the compression algorithm can improve the sampling rate and reduce the consumption of network bandwidth on the basis of ensuring data information [8]. Image encryption algorithm refers to the processing and transformation of pixel points to make the useful information in the original image hidden. The common image encryption algorithms include confusion and diffusion, which is to encrypt the image by changing the position of the pixel value of the pixel matrix or the pixel value of the whole image.

This study introduced compression sensing technology to process the image encryption algorithm, compared the image processing problem of agricultural environment with the information encryption process, and introduced blockchain technology to encrypt the

information and ensure the security of the information. The results from this research would provide guarantee and theoretical support for the improvement of agricultural environment and agricultural production.

Materials and methods

Compressed sensing fusion image based on adaptive algorithm

This study optimized the Sparsity Adaptive Matching Pursuit (SAMP) algorithm in compressed sensing theory to achieve the optimal selection of measurement matrix and sensor matrix and improve the reconstruction quality of the algorithm itself. There are nine kinds of sensing matrices commonly used in compressed sensing, most of which have large randomness. Their storage space is limited and easier to be limited than the application scenario. The Fourier matrix (FM) is a multidimensional variable, and its definition depends on the order. It has good reconstruction quality and orthogonality when performing linear measurement [9]. Therefore, the improved algorithm used in the study was FM matrix, and its calculation formula was shown in Formula (1).

$$\Phi_n = \begin{bmatrix} 1\ 1 & 1 & \cdots 1 \\ 1\ \xi & \xi^2 & \cdots \xi^{n-1} \\ 1\ \xi^2 & \xi^4 & \cdots \xi^{2(n-1)} \\ \cdots & & \\ 1\ \xi^{n-1} & \xi^{2(n-1)} & \cdots \xi^{(n-1)(n-1)} \end{bmatrix} \quad (1)$$

where n was the order. Φ was the element value of row j and column k of the FM matrix, where j and k were the subscript of the matrix. The product of two rows or two columns was 0, which had good orthogonality. The signal reconstruction rate of FM matrix was less disturbed by sparsity and had good reconstruction quality. To further met the applicability of Compressed Sensing (CS) theory in algorithm reconstruction [10], the sparsity adaptive matching pursuit algorithm based on FM matrix (FSAMP) was proposed. The algorithm used the comparison of the old and the new residuals as the criterion for selecting the number of atoms. The number of atoms was dynamically adjusted with the iteration step, which could effectively avoid atomic errors, so it could be adjusted adaptively. Because most of the detected image data had different time and type characteristics, it was difficult for a single image data to have a comprehensive understanding of the overall agricultural environment [11-13]. Non-down-sampling contourlet transform based on Nonsubsampled Contourlet (NSCT) transform and Sparse representation (SR) theory had good application effect in image fusion, so the research used this theory to fuse with CS to achieve image data fusion. Based on the low-frequency fusion system, sparse dictionary learning and low-frequency coefficient rules were applied to low-frequency sub-band images that contained a lot of energy information of the original image and had a small amount of geometric structure features. The gradient value of high-frequency sub-band was calculated by high-frequency fusion rules, and the image data was reconstructed to reduce the interference of noise information on the image. The flow chart of NSCT-SR-CS algorithm framework was shown in Figure 1. The CS image fusion algorithm based on NSCT and SR initially decomposed the original image into high-frequency sub-band and low-frequency sub-band and performed secondary decomposition. The low-frequency sparse fusion rule based on sparse dictionary was to obtain linear image information by sparse representation of the image. The divided low-frequency sub-band images were divided into blocks and arranged from top to bottom and from left to right to get the set step pixel blocks. The resulting blocks were rearranged and transformed. Formula (2) was then obtained after mean normalization.

$$\begin{aligned} &\overline{V^t{}_M} = V^t{}_M - \overline{V^t}{}_M \mathrm{W} \\ &\alpha^i{}_M = \arg\min_{\alpha} \|\alpha\|_0 \quad s.t. \left\| \overline{V^t{}_M} - D\alpha \right\|_2 < \varepsilon \end{aligned} \quad (2)$$

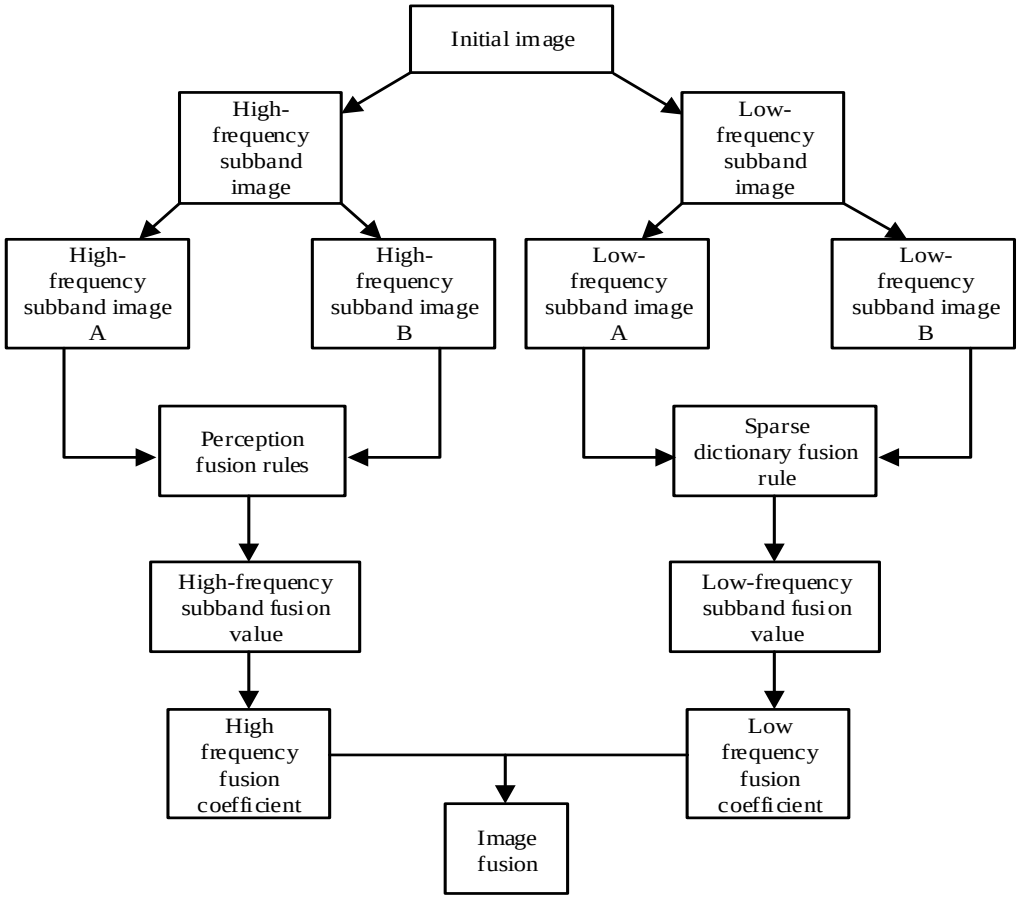

Figure 1. Flow chart of NSCT-SR-CS algorithm framework.

where $\overline{V^t{}_M}$ represented the second vector of the low-frequency coefficient of the detected image. *M* represented a different image. $\overline{V^t{}_M}$ was the average value of all elements in the vector. $\alpha^i{}_M$ represented the sparse coefficient of vector value. *D* was a sparse learning dictionary. Then the sparse coefficients were fused and expressed by sparse coefficient matrix, and the Formula (3) was obtained as follows.

$$V^i{}_F = D\alpha^i{}_F + \overline{V^t}{}_F \mathrm{W} \tag{3}$$

High-frequency subbands had rich edge information, and subband images at different scales had a lot of structural feature information. Therefore, when fusing its image information, it needed the change of its boundary gray level difference. The average gradient could better reflect the boundary information of the detected environment image, and the calculation formula of its average gradient value was shown as Formula (4).

$$G = \frac{\sum_{i=1}^{M-1}\sum_{j=1}^{N-1}\sqrt{\left(\frac{\partial f}{\partial x}\right)^2 + \left(\frac{\partial f}{\partial y}\right)^2}}{(M-1)(N-1)} \tag{4}$$

where *M* and *N* represented the impact of agricultural environmental monitoring. ∂f and ∂x were the gradient of the monitoring image in the horizontal and vertical directions, and were calculated by using Formula (5) below.

$$\begin{aligned} \frac{\partial f}{\partial x} &= f(x,y) - f(x+1,y) \\ \frac{\partial f}{\partial y} &= f(x,y) - f(x,y+1) \end{aligned} \tag{5}$$

The method of maximum absolute value was used to fuse the average gradient value of each high-frequency subband image to achieve the average gradient value of the fused high-frequency subband image.

When studying the number of atom selection and sparsity of the proposed improved algorithm, it was found that its initial step size played an important role in the reconstruction quality of the improved algorithm. When the step size was 5, the algorithm could give full play to its reconstruction efficiency. Therefore, the research used a Gaussian sparse signal with a signal length of 256 in the experiment process and set a unified control variable. The improved algorithm proposed in the study was used to compare with the regularized orthogonal matching pursuit (ROMP) algorithm, subspace pursuit (SP) algorithm, base pursuit (BP) algorithm, and Stagewise Weak Orthogonal Matching Pursuit (SWOMP) algorithm.

Image encryption algorithm based on blockchain technology

Based on elliptic curve cryptography, this study used discrete logarithm problem to encrypt the algorithm and ensure the security and efficiency under a certain key length. The curve of elliptic curve in the real number field was continuous and could not be encrypted, so it needed to be discretized and defined in the finite field [14]. The elliptic curve under the finite field could be expressed as follows.

$$y^2 = x^3 + ax + b \pmod{p} \quad (6)$$

where *P* was the point representing the prime number in the finite field. *a* and *b* were the numbers of finite fields. The element operation in a finite field could also be expressed as Formula (7).

$$h = E(F_p)/n \quad (7)$$

where *h* was the auxiliary factor. *n* was the order of the base point *G*. $E(F_p)$ was the curve in the finite field. *p* was the number of points in F_p. ECC encryption algorithm was an encryption process in a finite field, which was defined as Formula (8).

$$Q = kG \quad (8)$$

where *k* was a large number. *Q* and *G* were two points on the elliptic curve. The calculated value of *k* could be expressed as a discrete logarithm problem, which was difficult to deal with. In the encryption algorithm, *Q* and *G* were regarded as public key and private key. *k* was the base point of the elliptic curve. The encryption processing under elliptic curve encryption needed to ensure the integrity of elliptic curve, public key, base point, and ciphertext point, as well as private key, to realize the encryption processing of data information, which ensured the security of its transmission. Moreover, the encryption algorithm consumes less network bandwidth and has better processing speed [15]. The blockchain technology was introduced into the CS measurement matrix to encrypt it. The measurement matrix was used as the "key", and a Security Compressed Sensing based on Blockchain (SCSB) image encryption algorithm was proposed. Monte Carlo simulated numerical value with probability and statistics as the object, and mixed congruence method was used to generate random numbers, which were subject to uniform distribution.

$$\begin{cases} x_{k+1} = \mathrm{mod}(\lambda x_k + c, M) \\ \varepsilon_k = x_k / M \end{cases} \quad (9)$$

In Formula (9), x_k and ε_k were the chaotic factor. *c* was incremental. x_k and ε_k were non-negative numbers between 0 - 1. When the random number met Formula (10), the random number sampling could be transformed.

$$\begin{cases} (2\varepsilon_1 - 1)^2 + {\varepsilon_2}^2 \le 1 \\ X_f = \sqrt{-2\ln\varepsilon_1}\cos(2\pi\varepsilon_2) \\ Y_f = \sqrt{-2\ln\varepsilon_1}\sin(2\pi\varepsilon_2) \end{cases} \quad (10)$$

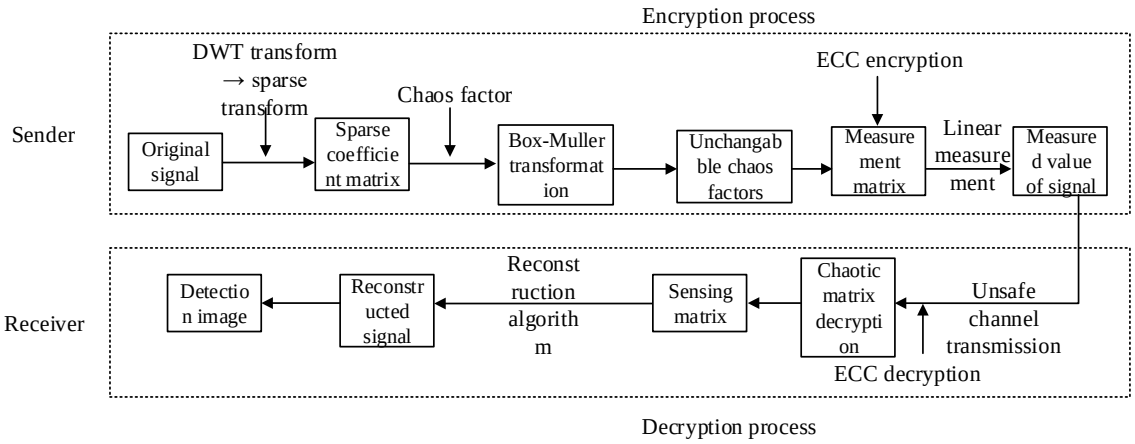

Figure 2. Blockchain-based secure compression-aware image encryption algorithm flowchart.

where $\mathcal{E}1$ and $\mathcal{E}2$ were random numbers. *X* and *Y* were random variables. The sample algorithm and the variables generated by the result were shown in the form of histogram. The mean value and mean square difference under the sampling method were compared with the standard normal distribution function value table. The transformed chaotic random number sequence was subject to Gaussian distribution and normal distribution, and the matrix subject to Gaussian distribution must satisfy the finite isometric property [16].

The measurement matrix in CS theory was constructed with the help of chaotic random sequence, and its form was shown in Formula (11).

$$\Phi_n = 1/\sqrt{M}\begin{bmatrix} X_0 & X_M & \cdots & X_{M(N-1)} \\ X_1 & X_{M+1} & \cdots & X_{M(N-1)+1} \\ \cdots & \cdots & \cdots & \cdots \\ X_{M-1} & X_{2M-1} & \cdots & X_{MN-1} \end{bmatrix} \quad (11)$$

where $\frac{1}{\sqrt{M}}$ was the normalization coefficient. *M* and *N* were the row and column data in the sequence. The pseudo-random number sequence constructed could effectively realize normalization processing. With the column as the benchmark, the random data in the sequence could establish a chaotic measurement matrix.

The implementation of the blockchain-based secure compression-aware image encryption algorithm was equivalent to the encryption processing of information. Figure 2 showed the process flow chart of the encryption algorithm. CS theory is equivalent to the encryption process of plaintext and the decryption process of ciphertext in the process of data signal acquisition and collection. The encryption effect of the algorithm depended on whether the measurement matrix could be cracked. The elliptic curve could effectively encrypt the measurement matrix that was regarded as a special "key" and added blockchain technology into the reconstruction algorithm to ensure the multiple guarantees and security of its data decryption.

Results and discussion

Performance comparison of secure compression aware encryption algorithms

Image fusion can make the spatiotemporal information expressed by multiple images better present on the same image and have higher image quality. It is used in image analysis, biological detection, and other fields. According to the level of information representation, this method can also be divided into three levels including pixel level, feature level, and decision level [17, 18]. Non-down-sampling contourlet

Table 1. Statistical results of reconstruction probability of different algorithms under different.

Sparsity	OMP	ROMP	SP	CoSaMP	BP	SWOMP	SAMP (s=5)	FSAMP (s=5)
10	100	100	100	100	100	100	100	100
15	100	70	100	100	100	100	100	100
20	100	13	100	100	100	100	100	100
25	100	0	100	100	100	100	100	100
30	100	0	100	100	100	100	100	100
35	100	0	100	100	100	99	100	100
40	100	0	99	98	98	87	100	100
45	80	0	88	55	84	52	100	98
50	0	0	65	0	50	17	99	95
55	30	0	32	0	15	4	92	94
60	0	0	5	0	3	0	75	84
65	8	0	0	0	0	0	22	21
70	0	0	0	0	0	0	0	0

Table 2. Reconstruction probability statistical results of different algorithms.

Measured number	OMP	ROMP	SP	CoSaMP	BP	SWOMP	SAMP (s=5)	FSAMP (s=5)
50	4	8	2	0	0	0	20	32
55	7	10	5	4	2	0	47	54
60	18	25	18	40	5	0	73	78
65	35	40	48	65	20	2	87	88
70	50	55	70	83	42	8	94	95
75	58	62	87	98	67	25	99	100
80	70	88	92	100	87	50	100	100
85	78	92	100	100	96	72	100	100
90	82	94	100	100	100	80	100	100
95	90	100	100	100	100	96	100	100
100	94	100	100	100	100	100	100	100

transform effectively guarantees the multiscale advantage of contourlet transform, and also eliminates the down-sampling step of its original two-level transform, so that it can be decomposed in multi-scale and multi-direction [19, 20]. The reconstruction probability of the algorithms in this study was in a downward trend in the later stage with the increase of the sparsity level (Table 1). The overall decline trends of OMP algorithm and ROMP algorithm were relatively obvious and sharp, indicating that their reconstruction probabilities were easily affected by the level of sparsity. The reconstruction probabilities of SP, CoSaMP, BP, and SWOMP were in the range of 90 to 100 when the sparsity level was 40, and the change was obvious in the later stage. The FSAMP algorithm proposed in the study showed a relatively stable performance in the early stage of the sparsity level with a step size of 5, and its overall average reconstruction probability was 84%. Its application effect was better than other algorithms. The reconstruction probability of the comparison algorithm was increasing with the increase of the number of measurements, and the reconstruction probability of SWOMP algorithm was 0 when the number of measurements was 55-65 (Table 2). The reconstruction probability of the improved FSAMP algorithm was higher than that of other algorithms under any number of measurements, and its reconstruction probability was basically stable and remained at 100 after the number of measurements reached 75. The reconstruction quality of the overall image was applied well.

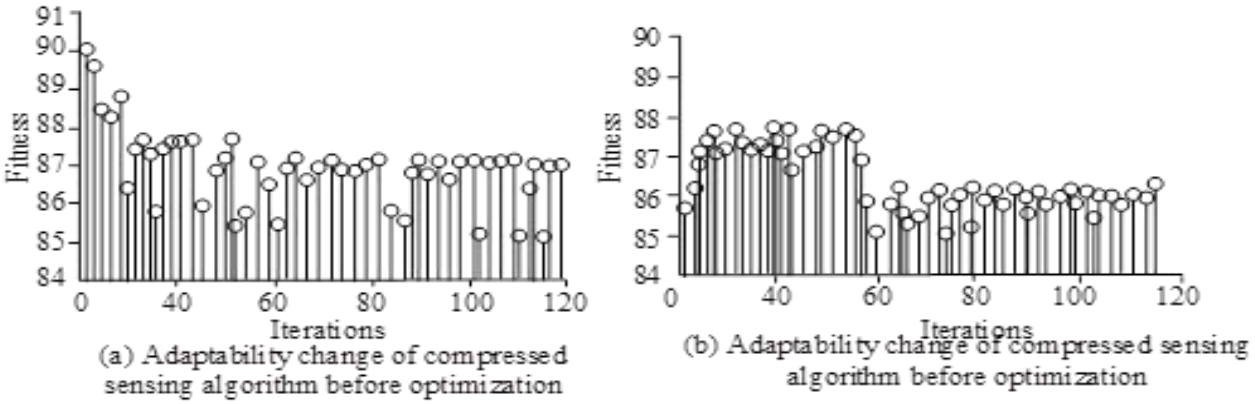

Figure 3. Adaptability changes before and after compression sensing algorithm optimization.

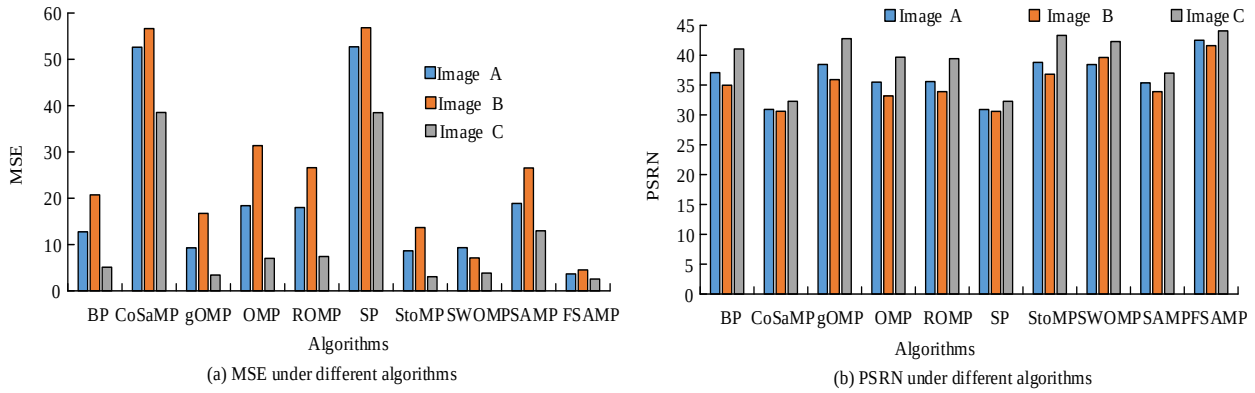

Figure 4. MSE and PSRN of image reconstruction under different algorithms.

Then, the algorithm adaptability and iterative performance of the algorithm in image reconstruction were sorted and analyzed. The fitness distribution of the model tended to be stable and basically remained at about 87 after the number of iterations of the parameters was 60 - 80 and after 90. Its fitness basically remained above 85 as the number of iterations increased (Figure 3a). The fitness change of model parameters could be basically bounded by 65 iterations, and the maximum fitness values before and after were close to 88 and 86, respectively (Figure 3b). The overall fitness change and processing efficiency of the algorithm were relatively stable. Then the agricultural environment image data with different scale characteristics were reconstructed, and the mean square error (MSE) and peak signal to noise ratio (PSNR) were used to measure the quality of image reconstruction. The comparison results of different algorithms were shown in Figure 4. The FSAMP algorithm demonstrated lower MSE and higher PSNR, indicating that its image restoration effect was significantly better than other algorithms. Specifically, the mean square error of the FSAMP algorithm in three different scales of influence images was small, all of which were less than 10%, which was not easily limited by image data. The larger the PSNR, the smaller the distortion of the image. The signal to noise ratios of FSAMP algorithm on image A, B, and C were 42, 41, and 45, respectively. The overall quality reconstruction effect of image information was good.

Evaluation and analysis of agricultural environmental monitoring image based on encryption algorithm

Table 3. Objective evaluation scores of different algorithms on image data processing.

Indicators	WT	LP	DWT	DTCWT	CVT	NSCT	LGP	Proposed method
Mean gradient	6.8011	7.6772	7.7238	7.5788	7.5907	7.5925	5.6825	7.7888
Edge strength	69.3582	78.0445	78.6105	76.8437	76.9942	77.0077	57.5680	78.6249
Information entropy	6.9183	7.2614	7.1732	7.1359	7.1405	7.1502	7.0008	7.3692
Standard deviation	32.6129	40.2949	37.9479	36.9873	37.0414	37.3841	33.2604	43.9347
Visual information fidelity	0.6018	0.9796	0.7405	0.9118	0.9008	0.9125	0.6512	0.9751

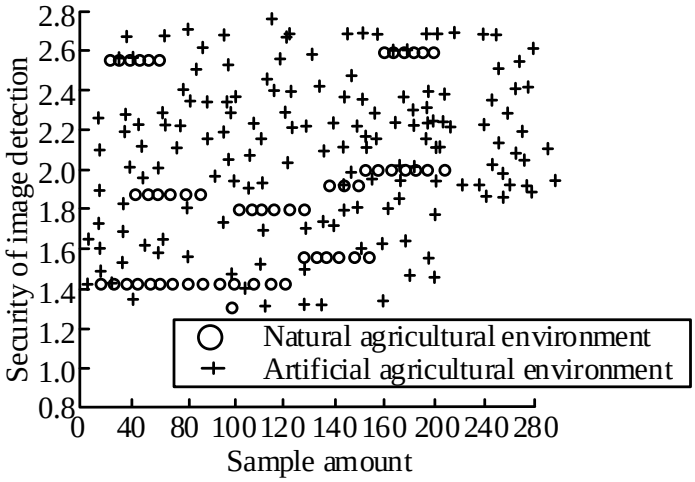

Figure 5. Detection security evaluation of two agricultural environments under the algorithm.

The evaluation standard of image quality is easily affected by subjective and objective factors. The subjective feelings of users and their role positioning will make their evaluation content biased and different. Therefore, this study used mathematical models to quantify the indicators to improve the reliability of their agricultural environment image data quality. The average gradient can reflect the processing effect of image data on small details. Edge intensity refers to the amplitude of the gradient of image edge points. The larger the value, the better the image fusion effect. Information entropy and standard deviation are important indicators to evaluate the information bearing degree and gray dispersion value of an image, and their value is proportional to the information richness and image contrast. Visual information fidelity can be used to judge the overall quality of the image. The fusion algorithm proposed in the study was compared with other adaptive fusion algorithms, weighted fusion rule algorithms, digital fusion algorithms, *etc*. to evaluate the processing effect of the fusion image. The data were statistically analyzed, and the results were shown in Table 3. The results showed that, when compared with other fusion algorithms, the fusion algorithm proposed in this study had higher scores in five dimensions including average gradient, edge strength, information entropy, standard deviation, and visual information fidelity as 7.7888, 78.6249, 7.3692, 43.9347, and 0.9751, respectively, which indicated that this method had high application effect in image fusion. The quality and integrity of image fusion were improved without distortion of its information. The DTCWT adaptive fusion algorithm is second only to the method proposed in this research in image processing effect.

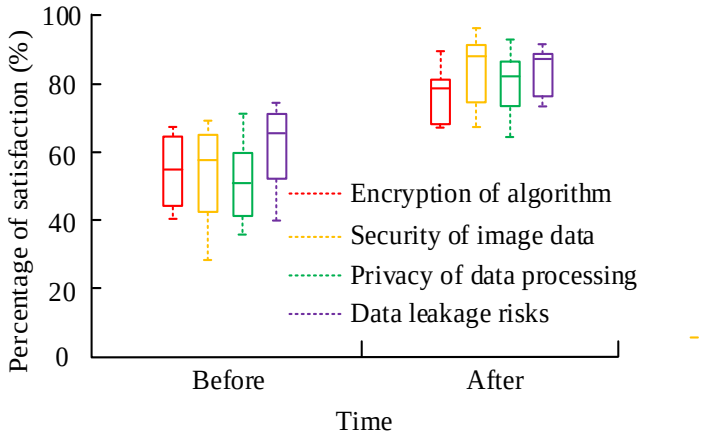

Figure 6. Expert scoring results of encryption algorithm application effect.

The security evaluation of the application effect of the two main agricultural environments under the encryption algorithm detection method adopted in the study was carried out. The numerical value of the ordinate represented the safety prediction capability (Figure 5). The values of the improved encryption algorithm in the evaluation of the security of the natural agricultural environment and the evaluation of the artificial agricultural environment were mainly clustered in 2.3 and 1.9, and the overall detection sample values were relatively clustered (Figure 3). This result demonstrated that this method could better ensure the effectiveness of its application effect. The experimental results and process of the algorithm applied to agricultural environment detection were evaluated by the expert group to prove the security of the algorithm. The satisfactions of the security compression encryption algorithm proposed in this study on the encryption of the algorithm, the security of image data, the privacy of data processing, and the risk of data leakage were all increased to varying degrees by comparing the scores before and after application (Figure 6) with the scores after application reached 80.12%, 89.23%, 82.16%, and 85.69%, respectively. The average satisfaction was more than 80%, which was higher than the score before application. The reason was that the addition of chaos factor and blockchain encryption technology made the encryption and decryption of data information required a large amount of computation, reduced the risk of its data being attacked by external illegal elements, and improved the security performance of image data to a certain extent.

Conclusion

The development of information technology of the Internet of Things makes the development of agriculture gradually incline to refinement and technicalization. The accuracy of agricultural information collection plays an indispensable role in the development of smart agriculture. The agricultural environment is an important infrastructure for agricultural production, but the original technical means make it easier to cause data leakage and image loss when transmitting agricultural environmental monitoring image data. Therefore, an image encryption algorithm based on security compression perception was proposed in this study, and the security of its image data detection was analyzed. The results showed that the algorithm proposed in this study had a relatively stable reconstruction probability in the early stage of sparsity, and its overall average reconstruction probability was relatively high. Its application effect was superior to SP algorithm, CoSaMP algorithm, BP algorithm, and SWOMP algorithm. Its reconstruction probability

was superior to other comparison algorithms under any number of measurements, and the overall reconstruction quality was good. When the algorithm proposed in this study reconstructed agricultural environment image data with different scale features, the MSE was low, and the overall MSE was less than 10%. Subsequently, the methods proposed in this study could also effectively ensure the quality of image fusion. Its scores in the five dimensions of average gradient, edge intensity, information entropy, standard deviation, and fidelity of visual information reached high values, respectively. The safety assessment of natural agricultural environment and artificial agricultural environment had been effectively realized.

References

1. Sodjinou SG, Mohammadi V, Mahama A, Gouton P. 2022. A deep semantic segmentation-based algorithm to segment crops and weeds in agronomic color images. Inf Process Agric. 9(3):355-364.
2. Liu DZ, Yang FF, Liu SP. 2021. Estimating wheat fractional vegetation cover using a density peak k-means algorithm based on hyperspectral image data. J Integr Agric. 20(11):2880-2891.
3. Chatterjee PS, Ray NK, Mohanty SP. 2021. Live Care: An IoT-based healthcare framework for livestock in smart agriculture. IEEE Trans Consum Electron. 67(4):257-265.
4. Bijandi M, Karimi M, Bansouleh BF, Knaap WV. 2021. Agricultural land partitioning model based on irrigation efficiency using a multi-objective artificial bee colony algorithm. Trans GIS. 25(1):551-574.
5. Yousefi-Babadi A, Bozorgi-Amiri A, Tavakkoli-Moghaddam R. 2022. Sustainable facility relocation in agriculture systems using the GIS and best–worst method. Kybernetes. 51(7):2343-2382.
6. Zha Z, Wen B, Yuan X, Ravishankar S, Zhou JT, Zhu C. 2022. Learning nonlocal sparse and low-rank models for image compressive sensing. arXiv e-prints. 40(1):32-44.
7. Chen J, Cheng Z, Chen W, Chen JQ, Zhan HP. 2022. Compressive sensing-based SAR imaging for undersampled echo. Microw Opt Technol Lett. 64(3):476-481.
8. Huang X. 2022. Offshore seismic exploration based on compressive sensing. Geophys Prospect Pet. 58(2):162-175.
9. Xiong M, Shin J, Chen L, Jaemin S. 2021. Accelerating the Bayesian inference of inverse problems by using data-driven compressive sensing method based on proper orthogonal decomposition. Electron Res Arch. 29(5):3383-3403.
10. Kourousias G, Billè F, Borghes R, Pascolo L, Gianoncelli A. 2021. Megapixel scanning transmission soft X-ray microscopy imaging coupled with compressive sensing X-ray fluorescence for fast investigation of large biological tissues. Analyst. 146(19):5836-5842.
11. Yousefi-Babadi A, Bozorgi-Amiri A, Tavakkoli-Moghaddam R. 2022. Sustainable facility relocation in agriculture systems using the GIS and best–worst method. Kybernetes. 51(7):2343-2382.
12. Zolfaghary M. 2021. A model for the use of urban treated wastewater in agriculture using multiple criteria decision making (MCDM) and geographic information system (GIS). Agric Water Manag. 243:106490.
13. Xu S, Wang X, Ye X. 2022. A new fractional-order chaos system of Hopfield neural network and its application in image encryption. Chaos Solitons Fractals. 157:111889.
14. Achour M, Hassani MI, Benhedid H, Brahim AH. 2021. Using GIS and geostatistical techniques for mapping piezometry and groundwater quality of the Albian aquifer of the M'zab Region, Algerian Sahara. Int J Geosci. 12:253-279.
15. Hang S, Li J, Xu X, Lyu Y, Li Y, Gong HR. 2021. An optimization scheme of balancing GHG emission and income in circular agriculture system. Sustainability. 13(13):7154.
16. Musse A, Massoud O, Ghanem KM, Ghanem KM. 2021. Response of eggplant to irrigation water quality, fertilization and organic extracts under urban agriculture system. Al-Azhar J Agric Res. 46(1):1-19.
17. Parvaz R, Yengejeh YK, Behroo Y. 2022. A new 4D chaos system with an encryption algorithm for color and grayscale images. Int J Bifurcat Chaos. 32(14): 2250214.
18. Deksissa T, Trobman H, Zendehdel K, Azam H. 2021. Integrating urban agriculture and stormwater management in a circular economy to enhance ecosystem services: Connecting the dots. Sustainability. 13(15):8293.
19. Twumasi YA, Ning ZH, Namwamba JB, Asare-Ansah A, Merem EC, Yeboah HB. 2022. Bioenergy crops as a promising alternative to fossil fuels in Louisiana: A geographic information system (GIS) perspective. J Sustain Bioenergy Sys. 12(4):57-81.
20. Oluwajuwon TV, Alo AA, Ogana FN, Adekugbe O. 2021. Forest cover dynamics of a lowland rainforest in southwestern Nigeria using GIS and remote sensing techniques. J Geogr Inf Syst. 13(2):83-97.